

Vibrational spectroscopy of fluid N₂ up to 34 GPa and 4400 K

S. C. Schmidt, D. S. Moore, and M. S. Shaw

Los Alamos National Laboratory, Los Alamos, New Mexico 87545

(Received 7 July 1986)

Single-pulse multiplex coherent anti-Stokes Raman scattering (CARS) was used to observe the vibrational spectra of liquid N₂ shock compressed to several pressures and temperatures up to 34 GPa and 4400 K. Vibrational frequencies, peak Raman susceptibilities, and Raman linewidths were determined for the fundamental and several excited-state transitions by comparing experimental spectra to synthetic spectra calculated using a semiclassical model for CARS intensities. The question of excited-state populations in the shock compressed state is addressed.

Recently there have been numerous papers discussing the high-pressure, high-temperature behavior of N₂. There have, however, been no measurements of the N₂ vibrational frequencies in the dense fluid state at temperatures sufficiently great to result in excited-state transitions. Such data would be of enormous value both to characterize the intramolecular potential function and possibly to verify directly the existence of dissociation. Measurements of ground and excited-state vibrational transition intensities could also provide an upper-limit estimate for the N₂ dense-phase fluid-vibrational relaxation time.

Reported here are measured frequencies, relative-peak third-order susceptibilities, and spectral half-widths of the fundamental and several excited vibrational transitions of diatomic N₂ at several pressures and temperatures up to 34 GPa and 4400 K. The pressure-temperature states were achieved by dynamic compression techniques and the vibrational spectra were measured using coherent anti-Stokes Raman scattering (CARS). The experimental apparatus has been described previously.^{1,2} Briefly, a projectile launched by a two-stage light-gas gun dynamically compressed a sample in a target designed to reflect the CARS signal back out through an optical aperture. The cryogenic target assembly used to condense and hold liquid N₂ for these experiments has been described elsewhere,³ but was modified to include a highly polished 304 stainless-steel target plate at the front and a 6.3-mm-diam quartz or lithium fluoride window at the rear. Impactor and target plate thicknesses were chosen, and pin assemblies were installed in the ~1.5-mm-long liquid-N₂ sample, so as to insure that rarefaction waves would not compromise the one-dimensional character of the compression in the region observed optically. Single-shock velocities were conservatively measured to ±5% and the initial pressure and temperature of the liquid-N₂ sample were determined to ±0.1 psi (absolute) and ±1 K, respectively. Initial sample densities were taken from Jacobsen *et al.*⁴ The N₂ samples were condensed from gaseous N₂ (purity greater than 99.9%).

In order to take advantage of the broader gain profile of the laser dye DCM (Exciton Chemical Company) (~600 cm⁻¹ versus ~200 cm⁻¹ for Rhodamine 590 previously

used), it was used in the broadband dye laser, to produce Stokes frequencies from 627 to 645 nm. The pump frequency in the CARS process was obtained by using approximately 40% of the Nd:YAG (YAG denotes yttrium aluminum garnet) laser output to pump a narrowband dye laser (Quanta-Ray PDL-1) at near 557 nm. Multichannel detection of the CARS signals was done using an intensified photodiode array (Tracor Northern model No. 6132) and analyzer (Tracor Northern model No. 6500). In addition, the broadband dye laser spectral profile was measured in each experiment using another 1-meter spectrometer, a photodiode array (Reticon model No. RL512S) and a transient digitizer (Biomation model No. 805).

Pressures, densities, and temperatures for the singly and doubly shocked regions were calculated using an effective spherical potential^{5,6} that has been shown to accurately reproduce both nonspherical molecular-dynamics simulations and experimental Hugoniot and brightness-temperature data. The calculated results are presented in Table I along with the initial conditions for each experiment. Doubly shocked states are inferred from impedance matching of the N₂ shock, at the measured shock velocity, reflecting off the known window material assuming the theoretical equation of state for N₂. The equation-of-state parameters for quartz and lithium fluoride are from published data.⁷ Based on the previously stated experimental errors, the estimated uncertainties are as follows: pressure ±1 GPa, density ±0.03 kg/m³, and temperature ±300 K for the first shock; and pressure ±2 GPa, density ±0.05 kg/m³, and temperature ±300 K for the reflected shock. The size of the uncertainties is dominated by the experimental uncertainty in the shock velocity. For comparison, Ross and Ree's⁸ corresponding states potential leads to pressures and densities within the above uncertainties and an upward temperature shift of 350 to 500 K depending on shock strength.

CARS (Refs. 9–14) occurs as a four-wave parametric process in which three waves, two at a pump frequency ω_p and one at a Stokes frequency ω_s , are mixed in a sample to produce a coherent beam at the anti-Stokes frequency, $\omega_{AS} = 2\omega_p - \omega_s$. The efficiency of this mixing is greatly enhanced if the frequency difference $\omega_p - \omega_s$ coincides with the frequency of a Raman-active mode of the sam-

TABLE I. Summary of shock conditions and spectroscopic parameters. (P denotes pressure in units of GPa, ρ denotes density in units of kg/m^3 , T denotes temperature in units of K, v denotes velocity in units of km/s , and ω_p is in units of cm^{-1} .)

Initial Conditions	Single-shock experiment					Double-shock experiment				
	Transition	ω_j (cm^{-1})	$\frac{\chi_j^{\text{pk}}}{\chi^{\text{NR}}}$	Γ_j (cm^{-1})		Transition	ω_j (cm^{-1})	$\frac{\chi_j^{\text{pk}}}{\chi^{\text{NR}}}$	Γ_j (cm^{-1})	
$P=0.003$ $\rho=0.78$ $T=82.9$ $\omega_p=17947.4$	Not shocked	0-1	2328.1	600.0	0.029					
$P=0.003$ $\rho=0.78$ $T=83.9$ $\omega_p=17948.4$	$P=9.3$ $\rho=1.53$ $T=2015$ $v=4.92$	0-1 1-2	2343.5 a	13.2 a	2.5 a	$P=14.4$ $\rho=1.73$ $T=2277$	0-1	2356.0	13.0	2.6
$P=0.003$ $\rho=0.783$ $T=82.9$ $\omega_p=17948.4$	$P=10.2$ $\rho=1.56$ $T=2196$ $v=5.11$	0-1 1-2 2-3	2344.7 2317.0 2287.2	12.5 5.6 2.4	2.6 2.6 2.6	$P=15.8$ $\rho=1.77$ $T=2480$	0-1 1-2 2-3	2356.4 2327.0 2297.0	12.4 6.7 2.2	2.7 2.7 2.7
$P=0.003$ $\rho=0.782$ $T=83.1$ $\omega_p=17947.4$	$P=15.6$ $\rho=1.69$ $T=3521$ $v=6.09$	0-1 1-2 2-3 3-4 4-5	2351.3 2323.2 2297.5 2269.5 2242.1	0.80 0.65 0.50 0.24 0.13	3.5 3.5 3.5 3.5 3.5	$P=34.4$ $\rho=2.13$ $T=4444$	0-1 1-2 2-3 3-4 4-5	2366.9 2338.3 2310.0 2281.5 2252.8	0.61 0.65 0.43 0.28 0.14	6.0 6.0 6.0 6.0 6.0

^aInsufficient signal-to-noise ratio to observe excited-state transitions.

ple. The intensity of the beam at ω_{AS} is given by

$$\begin{aligned}
 I_{\text{AS}} \propto \sum_i \frac{\omega_{\text{AS}}^2 I_p^2 I_S (N_i L_i)^2}{n_p^2 n_S n_{\text{AS}}} \left[\frac{n_{\text{AS}}^2 + 2}{3} \right]^2 \\
 \times \left[\frac{n_S^2 + 2}{3} \right]^2 \left[\frac{n_p^2 + 2}{3} \right]^4 \\
 \times \left[\left(\sum_j \frac{\Gamma_j \chi_j^{\text{pk}} (\omega_j - \omega_p + \omega_S)}{(\omega_j - \omega_p + \omega_S)^2 + \Gamma_j^2} + \chi^{\text{nr}} \right)^2 \right. \\
 \left. + \left[\sum_j \frac{\Gamma_j^2 \chi_j^{\text{pk}}}{(\omega_j - \omega_p + \omega_S)^2 + \Gamma_j^2} \right]^2 \right] \quad (1)
 \end{aligned}$$

and

$$\Gamma_j \chi_j^{\text{pk}} \frac{h}{2\pi c^4} \omega_p \omega_S^3 = \left(\frac{d\sigma}{d\Omega} \right)_j (\rho_j - \rho_k), \quad (2)$$

where h is Planck's constant, c is the speed of light, and n_{AS} , n_S , and n_p are the refractive indices at ω_{AS} , ω_S , and ω_p , respectively. I_p and I_S are the incident intensities of the pump and Stokes beams, respectively. $N_i L_i$ corresponds to the Lagrangian density of the i th layer, and the sum is over noninterfering layers. χ^{nr} is the nonresonant susceptibility, χ_j^{pk} is the peak third-order susceptibility, Γ_j is the half-width at half maximum linewidth, and $(d\sigma/d\Omega)_j$ is the spontaneous Raman cross section of the j to k vibrational transition. ρ_j is the number density in vibrational level j . The sum on j is over transitions. Equations (1) and (2) hold only in the case of no electronic resonance enhancement.¹⁴

Phase matching is assumed to be experimentally optimized in the ambient sample for the focusing conditions used. The dispersion in the sample is assumed to linearly scale with the increase in refractive index due to volume compression according to the empirical relation $n = 1.22 + 0.52(1 - V/V_0)$.¹⁵ V/V_0 is the relative volume due to compression and 1.22 is the approximate index of refraction of ambient liquid N_2 .¹⁶ Linear scaling of the dispersion results in the same phase-matching angle at all compressions. These refractive indices are also used in the local-field correction terms of Eq. (1).

The observed single-pulse CARS spectra of ambient pressure and six (three experiments) dynamically compressed states of liquid nitrogen are shown in Fig. 1. Because of timing constraints and the desire to have no unshocked sample at the time the laser pulses arrived, the shock wave in all three experiments has reflected off of the rear window back into the once-shock-compressed sample, producing a doubly shocked region. Because the ambient liquid- N_2 Raman linewidth is sufficiently narrow¹⁷⁻¹⁹ and because the line broadening with pressure is observed here to be sufficiently slow, spectral features from both the singly (denoted in Fig. 1 by asterisks) and doubly (arrows) shocked regions are clearly observed.

Wavelength calibrations ($\pm 2\text{cm}^{-1}$) were all done using vacuum wavelengths.²⁰ The narrow-band dye laser was placed near or in coincidence with the 17947.4-cm^{-1} transition of Kr, the broadband dye laser was calibrated versus the 15615.2- and 15953.5-cm^{-1} transitions of Ne, and the intensified diode array was calibrated using the 19931.9- and 20311.6-cm^{-1} transitions in He and the 19844.6-cm^{-1} transition of Ne; all of which were ob-

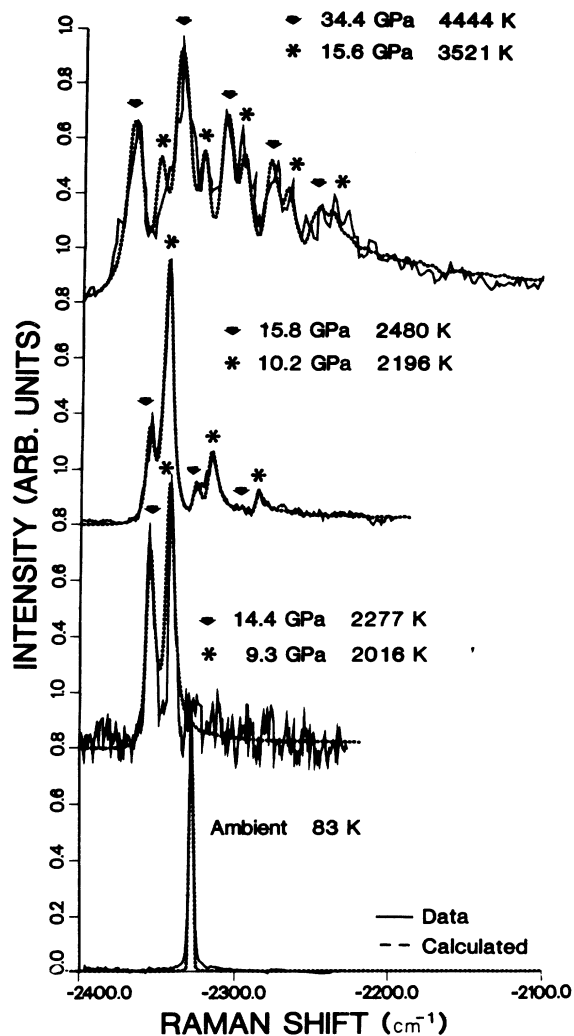


FIG. 1. Experimental and computed spectra for high-pressure and high-temperature N₂.

tained from standard calibration lamps. The spectral-slit-function of the spectrometer-photodiode array combination was also measured using the 19931.9-cm⁻¹ line of He and a 100- μ m-wide entrance slit. A good representation of this slit function was obtained by use of a 2.9-cm⁻¹ full width at half maximum triangle. The spectral profile of the narrow-band laser was accurately measured and was fit best by a Gaussian with 1.3 cm⁻¹ width at 1/e amplitude.

The transition frequencies, linewidths, and peak cross sections presented in Table I were obtained from the spec-

tra in Fig. 1 by fittings with synthetic spectra calculated using Eq. (1) and convolved with the 2.9-cm⁻¹-triangular slit function. Because the spectral fittings were accomplished primarily by visual inspection and the number of spectra that were fit is small, an accurate statement cannot be made about the errors in $\chi_j^{\text{pk}}/\chi_j^{\text{nr}}$ and Γ_j . A conservative estimate of the error is a factor of 2 of the stated value.

Experimental results²¹⁻²⁴ show that the dense fluid-N₂ vibrational relaxation time decreases from several seconds at atmospheric pressure to approximately 0.2 ms at 0.3 GPa. Because these times are long it is unclear whether, for the shock pressures and temperatures given in Table I, the relaxation time will decrease sufficiently rapidly (to ≈ 50 ns) to enable equilibration of the vibrational levels in the shock-compressed region interrogated by CARS. It is also unclear what effect impurities will have on the density dependence of the relaxation time.^{23,24} Ratios of Eq. (2) for excited-state to fundamental transitions were used to explore the possibility of a non-Boltzmann population distribution for the excited states. The right-hand-side ratios were calculated using the harmonic-oscillator approximation for the variation of the Raman cross section with vibrational level ($d\sigma/d\Omega$)_{*j*} $\propto (j+1)$, and assuming a Boltzmann distribution for ρ_j . For all transitions, the ratios of the left side determined using the experimental values stated in Table I, agreed with the values calculated for the right-hand side. This suggests that, subject to the stated approximations, vibrational equilibration occurs faster than ≈ 50 ns at these pressures and temperatures. However, because of the large uncertainties in the experimental quantities (particularly the measured peak third-order susceptibilities and the Raman half-widths), this conclusion does not yet merit a definite statement.

In summary, at pressures up to 34 GPa and 4400 K, N₂ exists as a molecular fluid with vibrational frequencies, third-order susceptibilities, and half-widths given in Table I. For the observed transitions and within the uncertainty in the measured frequencies, the spacings between transitions are constant and do not differ from those expected based on gas-phase data.²⁵ Also, higher vibrational states are excited in ≤ 50 ns. Within the limits of the approximations used and experimental error, thermal equilibration of these levels is suggested.

The authors wish to thank Charles Caldwell, John Chavez, John Chacon, Rick Eavenson, James Esparza, Joseph Fritz, Concepcion Gomez, Vivian Gurule, Robert Livingston, Janet Neff, George Pittel, Dennis Price, Terry Rust, and Dennis Shampine for their invaluable work in obtaining the results presented in this paper. They are especially grateful to J. W. Shaner for his encouragement and support of this work.

¹D. S. Moore, S. C. Schmidt, and J. W. Shaner, Phys. Rev. Lett. **50**, 1819 (1983).

²S. C. Schmidt, D. S. Moore, D. Schiferl, M. Châtelet, T. P. Turner, J. W. Shaner, D. L. Shampine, and W. T. Holt, in *Advances in Chemical Reaction Dynamics*, Proceedings of

Nato Advanced Study Institute, Iraklion, Greece, 1985, edited by P. M. Rentzepis and C. Capelles (D. Reidel, Dordrecht, 1986), p. 425.

³W. J. Nellis and A. C. Mitchell, J. Chem. Phys. **73**, 6137 (1980).

- ⁴R. T. Jacobsen, R. B. Stewart, R. D. McCarty, and H. J. M. Hanley, Natl. Bur. Stand. (U.S.) Tech. Note No. 648 (U.S. GPO, Washington, D.C., 1973).
- ⁵M. S. Shaw, J. D. Johnson, and B. L. Holian, Phys. Rev. Lett. **50**, 1141 (1983).
- ⁶J. D. Johnson, M. S. Shaw, and B. L. Holian, J. Chem. Phys. **80**, 1279 (1984).
- ⁷S. P. Marsh, *LASL Shock Hugoniot Data* (University of California Press, Berkeley, California, 1980); W. J. Carter, High Temp. High Pressures **5**, 313 (1973).
- ⁸M. Ross and F. H. Ree, J. Chem. Phys. **73**, 6146 (1980).
- ⁹J. W. Nibler and G. V. Knighten, in *Raman Spectroscopy of Gases and Liquids*, edited by A. Weber (Springer-Verlag, Berlin, 1979), p. 253.
- ¹⁰P. D. Maker and R. W. Terhune, Phys. Rev. **137**, A801 (1965).
- ¹¹N. Bloembergen, H. Lotem, and R. T. Lynch, Jr., Indian J. Pure Appl. Phys. **16**, 151 (1978).
- ¹²N. Bloembergen, *Nonlinear Optics* (Benjamin, Reading, MA, 1965).
- ¹³S. A. J. Druet and J. P. E. Taran, Prog. Quantum Electron. **7**, 1 (1981).
- ¹⁴W. B. Roh, P. W. Schreiber, and J. P. E. Taran, Appl. Phys. Lett. **29**, 174 (1976).
- ¹⁵K. Vedam, in *Critical Reviews in Solid State and Materials Sciences*, edited by D. E. Schuele and R. W. Hoffman (CRC, Boca Raton, FL, 1983), p. 1.
- ¹⁶J. F. Ely and G. C. Straty, J. Chem. Phys. **61**, 1480 (1974).
- ¹⁷W. R. L. Clements and B. P. Stoicheff, Appl. Phys. Lett. **12**, 246 (1968).
- ¹⁸M. J. Clouter and H. Kiefte, J. Chem. Phys. **66**, 1736 (1977).
- ¹⁹S. A. Akhmanov, F. N. Gadjiev, N. I. Koroteev, R. Yu. Orlov, and I. L. Shumay, Appl. Opt. **19**, 859 (1980).
- ²⁰*M.I.T. Wavelength Tables*, prepared by F. M. Phelps III (MIT Press, Cambridge, MA, 1982), Vol. II.
- ²¹M. Châtelet, J. Kieffer, and B. Oksengorn, Chem. Phys. **79**, 413 (1983).
- ²²M. Châtelet and J. Chesnoy, Chem. Phys. Lett. **122**, 550 (1985).
- ²³C. Manzanares and G. E. Ewing, J. Chem. Phys. **69**, 1418 (1978).
- ²⁴D. W. Chandler and G. E. Ewing, J. Chem. Phys. **73**, 4904 (1980).
- ²⁵G. Herzberg, *Spectra of Diatomic Molecules* (Van Nostrand Reinhold, New York, 1950).